ACS SENSORS

Article

Cite This: ACS Sens. 2019, 4, 3023−3033

pubs.acs.org/acssensors

Detecting Gold Biomineralization by *Delftia acidovorans* Biofilms on a Quartz Crystal Microbalance

Riccardo Funari,*[,†] Rosa Ripa,[†] Bill Söderström,[‡] Ulf Skoglund,[‡] and Amy Q. Shen*[,†]

[†]Micro/Bio/Nanofluidics Unit and [‡]Structural Cellular Biology Unit, Okinawa Institute of Science and Technology Graduate University, 1919-1 Tancha, Onna-son, Kunigami-gun, Okinawa 904-0495, Japan

Supporting Information

ABSTRACT: The extensive use of gold in sensing, diagnostics, and electronics has led to major concerns in solid waste management since gold and other heavy metals are nonbiodegradable and can easily accumulate in the environment. Moreover, gold ions are extremely reactive and potentially harmful for humans. Thus, there is an urgent need to develop reliable methodologies to detect and possibly neutralize ionic gold in aqueous solutions and industrial wastes. In this work, by using complementary measurement techniques such as quartz crystal microbalance (QCM), atomic force microscopy, crystal violet staining, and optical microscopy, we investigate a promising biologically induced gold biomineralization process accomplished by biofilms of bacterium *Delftia acidovorans*. When stressed by Au^{3+} ions, *D. acidovorans* is able to neutralize toxic soluble gold by excreting a nonribosomal peptide, which forms extracellular gold nanonuggets via complexation with metal ions. Specifically, QCM, a surface-sensitive transducer, is employed to quantify the production of these gold complexes directly on the *D. acidovorans* biofilm in real time. Detailed kinetics obtained by QCM captures the condition for maximized biomineralization yield and offers new insights underlying the biomineralization process. To the best of our knowledge, this is the first study providing an extensive characterization of the gold biomineralization process by a model bacterial biofilm. We also demonstrate QCM as a cheap, user-friendly sensing platform and alternative to standard analytical techniques for studies requiring high-resolution quantitative details, which offers promising opportunities in heavy-metal sensing, gold recovery, and industrial waste treatment.

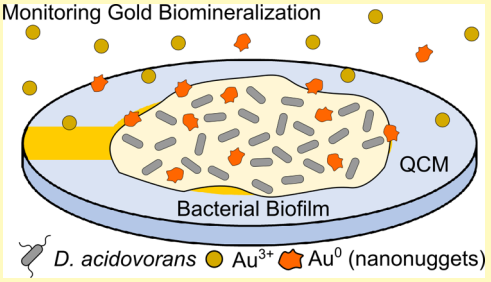

KEYWORDS: *D. acidovorans, quartz crystal microbalance, biomineralization, bacterial biofilm, heavy-metal detection*

Unique biocompatibility, tunable surface functionalities, optical properties, and controlled drug-release capability make gold nanoparticles (AuNPs) suitable for applications ranging from sensing to medical diagnostics.[1] Solid gold has also found wide applications in the electronic industry. However, the extensive use of noble metals has caused difficulty in solid waste management since gold and other heavy metals are non-biodegradable and accumulate in the environment.[2] Moreover, intermediate products in gold processing and precursors of AuNPs synthesis, such as Au(I) and Au(III) compounds, are extremely reactive and potentially harmful for humans.[3,4] For instance, Au(III) salts, such as gold chloride ($AuCl_3$), can damage the liver, kidney, and the peripheral nervous system.[5] In addition, Au^{3+} ions are toxic to the majority of bacteria.[6] Interestingly, microbial biofilms, clusters of microorganisms closely packed on a solid surface within a self-produced matrix of extracellular polymeric substances (EPS),[7] have been observed on the surface of gold nuggets, suggesting that some microorganisms have developed specific resistance mechanisms to both solid and soluble gold, motivating potential applications in metal detoxification.[8] Genome sequencing of gold nugget microbiota has revealed that *Cupriavidus metallidurans* and *Delftia acidovorans* are the dominant organisms within such communities, comprising over 90% of the bacteria in these biofilms.[9] Indeed, these microorganisms respond to the presence of toxic and soluble gold by activating specific metabolic pathways that reduce ionic gold to solid gold, in the form of the so-called "nanonuggets".[10] When stressed by Au^{3+} ions, *D. acidovorans* produces the nonribosomal extracellular peptide delftibactin, which forms gold particles via metal complexation to protect the microorganism against toxic soluble gold.[10] This biologically induced biomineralization process can be exploited in a wide range of applications, such as environmentally friendly cell-based synthesis of AuNPs, and gold recovery from electronic waste and environmental matrices such as seawater.[11] Moreover, the capability of microorganisms such as *D. acidovorans* to neutralize heavy-metal ions in solution offers unique opportunities to develop alternative cell-based biosensors for heavy-metal detection. Recently, biosensors have incorporated whole cells, enzymes, and oligonucleotides for heavy-metal detection.[12] However, whole cells have shown advantages over proteins and nucleic acids: they are cheaper to use, easier to maintain, and have better tolerance against environmental changes. For these reasons, whole cells have

Received: August 16, 2019
Accepted: October 21, 2019
Published: October 21, 2019

DOI: 10.1021/acssensors.9b01580
ACS Sens. 2019, 4, 3023−3033

found applications in the detection of heavy metals such as lead,[13] cadmium,[14] copper,[15] chromium,[16] and nickel[17] using either optical or electrochemical transduction principles.

Since conventional laboratory approaches (e.g., inductively coupled plasma mass spectrometry) to quantify metal ions rely on complex and expensive techniques,[18] they are not well suited for real-time and routine measurements on microorganisms. Therefore, the detailed characterization of gold biomineralization from bacteria such as *D. acidovorans* is still lacking, while such information is critical in designing and optimizing the gold-recovery process involving microorganisms. For example, native conditions experienced by *D. acidovorans*, i.e., biofilm formation on solid gold surfaces, have never been explored.

Acoustic sensors, specifically quartz crystal microbalances (QCM), have received increasing attention in sensing due to their cost-effectiveness and flexibility in investigating molecular recognition and surface phenomena.[19,20] QCM measures the adsorbed/deposited mass on its gold-sensitive surface by monitoring variations of the oscillation frequency of a quartz crystal resonator with a resolution of ≈ ng/Hz. In addition, this device has been used to estimate the stiffness of adsorbed materials by measuring the energy dissipation factor (D).[21] Therefore, QCM has been utilized as a reliable tool to track various biological processes involving DNA hybridization,[22,23] antigen−antibody binding,[24,25] and prokaryotic and eukaryotic cell adhesion responses to different stimuli.[26,27] QCM also offers a wide range of possibilities in terms of the sensor surface (e.g., gold, silver, titanium, copper, etc.) with additional coatings (e.g., plastic, silicon oxide, etc.). In fact, QCM has been used as a sensor platform to monitor bacterial adhesion and various biofilm developmental stages in real time.[28−35]

Motivated by the possibility to detect heavy metals using microbial biofilms, we use label-free QCM to characterize *D. acidovorans* biofilm formation and detect Au^{3+} biomineralization on a gold-coated quartz QCM surface in real time. The QCM characterization of biofilm assembly is complemented by optical microscopy, atomic force microscopy (AFM) imaging, and crystal violet (CV) staining. Toxic effects of soluble gold on bacterial cells have been estimated through viability staining, while the biomineralization process is confirmed using a colorimetric assay.[36] Specifically, gold biomineralization by *D. acidovorans* is detected directly on the QCM surface by stressing its microbial biofilm with $AuCl_3$ solutions at various concentrations, with the sensor resonance frequency and energy dissipation signals being monitored for 14 h. To the best of our knowledge, this is the first study providing an extensive characterization of a gold biomineralization process by a bacterial biofilm and since QCM is an extremely sensitive mass sensor, it can be an excellent device to quantitatively detect the gold nanonuggets resulting from the Au^{3+} biomineralization, and consequently identify the experimental conditions to maximize the gold recovery and the production of nanonuggets.

MATERIALS AND METHODS

Chemicals. Crystal violet powder (C6158), gold (III) chloride trihydrate (520918), 3,3',5,5'-tetramethylbenzidine (TMB) (860336), sulfuric acid (258105), and hydrogen peroxide solution (216763) were purchased from Sigma-Aldrich. Live/Dead BacLight Bacterial Viability Kit (L13152) was purchased from Invitrogen. Poly(dimethylsiloxane) (PDMS) was purchased from Dow Corning (Japan). 1× phosphate-buffered saline (PBS) (pH 7.4) is used both as the biomineralization and washing buffer.

Bacterial Growth and Biomineralization Conditions. *D. acidovorans* (ATCC 15668) and *Escherichia coli* (WT MG1655, Lab collection) are streaked on Nutrient Agar (DB Difco, 213000) and LB agar (Sigma-Aldrich, L3022 and A1296) plates, respectively. Stocks of both strains are kept in glycerol at −80 °C. Single colonies are picked from their respective plates and used to inoculate 20 mL of either nutrient broth (NB, for *D. acidovorans*) or lysogenic broth (LB, for *E. coli*) and grown overnight (≈16 h) at 30 °C under continuous shaking (200 rpm).

Gold biomineralization conditions are examined by exposing the biofilm formed on the QCM gold surface to either NB or minimal medium (MM), consisting of M9 salts (Sigma-Aldrich, M6030) supplemented with 0.2% glucose [w/v], 0.1% casaminoacids [w/v], and 1 μg/mL thiamine.

Quartz Crystal Microbalance (QCM). The QCM device (openQCM Q-1) was purchased from Novaetech, Italy. Gold-quartz oscillators (QL0765) were purchased from I.E.V., Italy. They are AT-CUT quartz with a fundamental frequency of 10 MHz. Crystal and gold electrode diameters are 1.37 and 0.6 cm, respectively. The QCM gold-coated quartz substrates are cleaned using the "piranha solution", a 3:1 mixture of sulfuric acid (H_2SO_4) and 30% hydrogen peroxide (H_2O_2). Since the piranha solution is a strong oxidizing agent, it is commonly used in microelectronics to remove organic contaminants from substrates. In the fume hood, hydrogen peroxide is slowly poured in a glass beaker containing sulfuric acid, resulting in an extremely exothermic reaction. After the solution cools, QCM sensor substrates are immersed with steel tweezers in the reactive solution for about 2 min. Next, the substrates are washed with MilliQ water and dried with a gentle stream of nitrogen. This aggressive chemical treatment allows QCM sensor substrates to be reused up to 3−4 times.

Once the gold−quartz oscillator is mounted, the liquid sample is confined on the gold-sensitive surface via an open cell that allows sample volumes up to 200 μL. The cell is closed with a teflon cover and the whole sensing modulus is protected by a three-dimensional-printed cap containing a water reservoir. This is critical to prevent sample evaporation. Both resonance frequency and dissipation values are recorded in real time via the manufacturer's software. Data are then analyzed using OriginPRO 2017 (OriginLab).

Monitoring *D. acidovorans* Biofilm Formation using QCM. 200 μL of NB are loaded into the QCM chamber and 1 μL of the overnight bacterial culture (equal to an initial concentration of bacteria of about 2×10^7 CFU/mL) is then added to the QCM chamber when both the frequency and the dissipation signals are stable (this happens after about 1 h from the loading of the NB). Both resonance frequency and dissipation are monitored for 24 h at room temperature (25 °C). All measurements are performed in triplicate.

Real-Time Optical Imaging of *D. acidovorans* Biofilm Formation. The gold-coated glass substrate for real-time microscopic characterization of *D. acidovorans* biofilm formation is prepared by depositing 15 nm of gold on a glass cover slip (Matsunami Micro Cover Glass, Japan, thickness 0.170 ± 0.005 mm) using an e-beam evaporator (KE604TT1-TKF1, Kawasaki Science) in a Class 1000 clean room. Before metal deposition, glass substrates are cleaned via sonication for 3 min in acetone and isopropanol. These conditions provide a continuous metal film similar to the gold-coated quartz surface of the QCM. The gold substrate is then bonded to a poly(dimethylsiloxane) (PDMS) slab via double-sided tape. A PDMS layer (6−7 mm thick) is prepared by pouring a 10:1 prepolymer/curing agent mixture (Dow Corning, Japan) in a petri dish. After degassing to remove air bubbles, the mixture is cured for 3.5 h at 60 °C. Then, 8 mm holes are punched using disposable biopsy punchers (Kai Medical, Japan) to create PDMS wells. Bacteria are grown under the same conditions as those described in the previous paragraph. Images are captured every 2 min over 24 h at 25 °C using a Leica thermal stimulated current SP8 confocal microscope operated in transmitted light mode.

Morphological Characterization of Microbial Biofilm using Atomic Force Microscopy. Microscopic characterization of *D. acidovorans* biofilm grown on QCM gold surfaces is performed using an atomic force microscope (Dimension ICON3 from Bruker, Japan) equipped with aluminum back-coated cantilevers (OTESPA-R3, Bruker, Japan) with nominal tip radius values ≈ 7 nm, spring constant $k \approx 26$ N/m, and resonance frequency $f_0 \approx 300$ kHz. The microbial

DOI: 10.1021/acssensors.9b01580
ACS Sens. 2019, 4, 3023−3033

biofilms are imaged in tapping mode with a scanning speed of 1 line/s and a relatively high-amplitude set-point ratio ($A_{sp}/A_{free} \approx 0.85$) to reduce the risk of tip contamination. Areas of 20×20 and 10×10 μm^2 are scanned with a resolution of 512 pixels per line. All of the measurements are performed in triplicate and image analysis is performed using NanoScope Analysis 1.8 software (Bruker).

Crystal Violet Staining. Crystal violet (CV) assay is widely used to quantify biofilm biomass.[37,38] We adopt the standard procedure to validate the results obtained with the QCM device at 24 h. In addition, we have used *E. coli* as a reference microorganism. *E. coli* is grown in LB, under similar conditions as *D. acidovorans*, with the detailed procedure included in the Supporting Information (SI).

Viability Staining. Live/Dead BacLight Bacterial Viability Kit is used to evaluate the decrease in bacterial vitality due to gold toxicity. It is based on bacterial staining using a mixture of SYTO 9 and propidium iodide dyes. Specifically, SYTO 9 provides green fluorescence and labels living bacteria, while propidium iodide, which emits in the red spectral region, labels dead cells. The *D. acidovorans* biofilm is stained directly on the QCM gold surface and the detailed protocol and information about the image analysis are reported in SI.

3,3′,5,5′-tetramethylbenzidine (TMB) Assay. Xia et al.[36] have demonstrated that 3,3′,5,5′-tetramethylbenzidine (TMB), a substrate commonly used in ELISA assays, can be used for quantifying Au^{3+} ions in solution. TMB is specifically oxidized by Au^{3+} ions, producing a charge-transfer complex that strongly absorbs light at 654 nm. Therefore, the TMB assay is used for independent validation of the gold biomineralization by *D. acidovorans* biofilm by estimating the amount of free Au^{3+} remaining in the solution in the QCM measurement cell over 14 h. First, a 2 mM indicator solution is prepared by dissolving TMB powder in a 4:1 mixture of ethanol and NaAc/HAc buffer 1 M at pH 3.5. The TMB solution is stored at 4 °C to prevent its degradation. To estimate the Au^{3+} content in a sample loaded in the QCM cell, we first calibrate the response of the assay using $AuCl_3$ samples in PBS. 10 μL of Au^{3+} sample is mixed with 2 μL of TMB solution. After 10 min of incubation at room temperature (25 °C), the absorbance spectrum between 500 and 800 nm is recorded using an UV−vis spectrophotometer (NanoDrop 2000). In particular, absorbance at 654 nm is plotted against the $AuCl_3$ concentration and used as a reference. The same procedure is performed on the biofilm supernatant at different times. Since some cells can also be captured while recovering the supernatant, continuing the biomineralization, and reducing the amount of Au^{3+} in solution, all samples are collected and then kept at 4 °C until reactant is added.

RESULTS AND DISCUSSION

Since it provides direct, nondisruptive, and real-time surface characterizations, QCM is a valuable tool to study biofilms and how they respond to different stimuli. Here, we use QCM to characterize the *D. acidovorans* biofilm formation on a gold-coated quartz surface of a QCM and examine how the bacteria respond to soluble gold at different concentrations. The experimental procedure and schematic of the biofilm development and gold biomineralization are illustrated in Figure 1. First, the bacteria grow for 24 h on the QCM surface (steps 1−3), forming a compact biofilm structure. After washing the biofilm with phosphate-buffered saline (PBS, step 4) to remove the residual culture medium, cells are stressed for ≈14 h with a $AuCl_3$ solution at concentrations ranging from 0.5 to 100 μM (step 5). This induces the production and secretion of delftibactin, which binds soluble gold to form an insoluble complex (step 6). Since *D. acidovorans* naturally grows on gold substrates, QCMs with gold-coated quartz sensors are well suited to study the biofilm formation and gold biomineralization of *D. acidovorans*. Finally, the interaction of *D. acidovorans* bacteria with the sensor surface does not produce any visible degradation of the gold electrode, as verified via AFM and

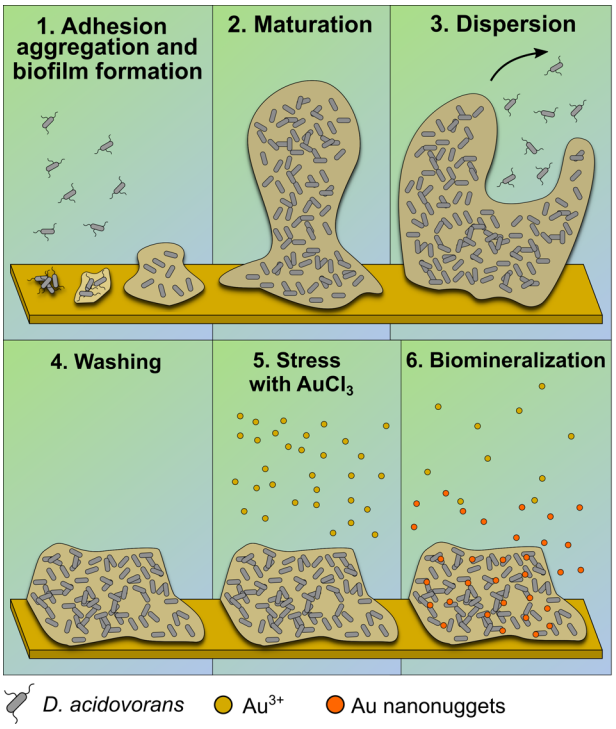

Figure 1. Stages of *D. acidovorans* biofilm development and gold biomineralization. The bacteria first grow for 24 h on the gold-coated quartz sensor surface of the QCM (from step 1 to 3), and then the biofilm is washed with PBS (step 4) and stressed with $AuCl_3$ for about 14 h (step 5). The exposure to soluble Au^{3+} ions induces the production of the nonribosomal peptide delftibactin, which neutralizes the ionic gold, creating the so-called nanonuggets (step 6).

scanning electron microscopy images (see SI and Figure S2 for more details).

Real-Time Monitoring of *D. acidovorans* Biofilm Formation with QCM and Optical Microscopy. A quartz crystal microbalance with dissipation monitoring (QCM-D) enables measurements of both the resonance frequency of the oscillating quartz and the energy dissipation associated with the material adsorbed on the sensor surface. While changes in the resonance frequency usually indicate an addition of mass on the QCM, variations in energy dissipation are related to the stiffness of the material in contact with the sensor surface. Many studies report a decrease in resonance frequency upon bacteria adhesion and biofilm formation, consistent with the standard Sauerbrey's model,[33,39] an empirical equation describing the direct proportionality between the decrease in the oscillation frequency of a piezoelectric crystal and the mass deposited on it. However, some other studies[29,40] show that adhesion of some bacteria can lead to an increase in the frequency over its original resonance value, which can be explained by the coupled−oscillator theory, in which the bacterium-resonator system simulates a pair of coupled oscillators.[41] The QCM signal transduction is determined by the interaction between bacterial cells and a surface, mediated by appendages such as pili, flagella, and curli,[42,43] and extracellular polymeric substances (EPS) components of biofilm matrix including polysaccharides, proteins, and extracellular DNA.[7] If bacteria are weakly bonded on the sensor surface, its oscillation frequency is much lower than its basal quartz frequency.[40] In this condition, the bond between cells and the sensor surface exerts a restoring force on the QCM, increasing its effective stiffness, and therefore its

DOI: 10.1021/acssensors.9b01580
ACS Sens. 2019, 4, 3023−3033

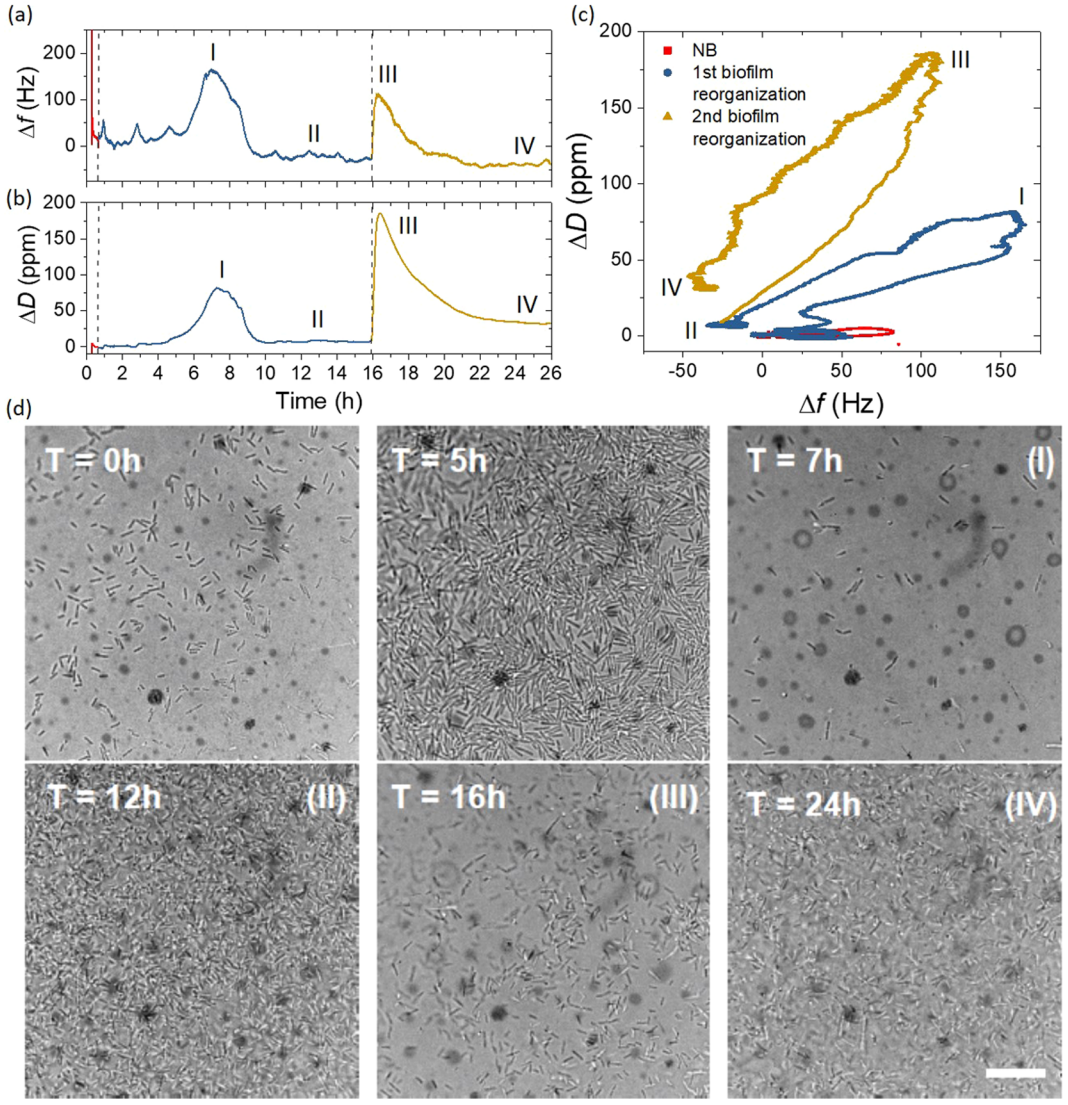

Figure 2. QCM sensorgrams of *D. acidovorans* growth on gold and optical images of the biofilm structure. Panels (a) and (b) show frequency and dissipation responses versus time, respectively. An initial stabilization in NB (red data), corresponding to protein adsorption on the gold sensor surface, is followed by a gradual increase in both frequency and dissipation (blue data). This peak (I) is a signature of bacterial reorganization on the gold sensor surface. Next, bond maturation of the cells onto the gold surface results in another stabilization regime for both frequency and dissipation (II). A second increase in both signals can be observed at about 16 h (yellow data, III), followed by a final stabilization (IV). While the first peak can be attributed to a rearrangement of the cell layer directly adhering to the gold surface, the second one is related to reorganization of the external part of the biofilm. These stages can be captured in the *Df*-plot (c), where the dissipation shift is plotted against the frequency change, and further validated in a sequence of images extracted from a time-lapse series of *D. acidovorans* grown on a 15 nm gold layer evaporated on a glass cover slip (d). Images of bacterial growth are captured every 2 min over ≈ 24 h at 25 °C (see SI video). In these conditions, biofilm reorganization occurs around 7 and 16 h. The scale bar represents 20 μm.

resonance frequency. On the other hand, when the cells adhere firmly to the sensor surface, the bacteria start to oscillate synchronously with the quartz, thus decreasing its resonance frequency as predicted by Sauerbrey's model.

D. acidovorans biofilm growth sensorgrams recorded at 25 °C (Figure 2a,b) display two reproducible characteristic peaks in its frequency and dissipation at about 7 ± 1 and 15 ± 1 h, which are associated with biofilm reorganization and bond maturation on the sensor surface and can be explained by the coupled−oscillator theory. After an initial incubation of the gold-coated quartz sensor with the nutrient broth (NB) culture medium (red line), inoculum was loaded into the QCM chamber. This led to a progressive increase in both frequency and dissipation (blue lines), which culminated with a first peak (I) at about 7 h, followed by a decrease and stabilization of both signals (II). This first peak describes the initial bacterium−sensor interaction where bacterial appendages and proteins on the cell membrane can lead to weak coupling between the bacteria and the QCM surface, producing an increase in frequency.[44] Next, adhered bacteria start to produce extracellular polymeric substances (EPS), leading to an increase in dissipation as well. When cells are firmly adsorbed on the QCM gold surface, the biofilm mass is coupled with the QCM sensor, resulting in a net negative shift in frequency and a positive variation in dissipation. Indeed, when the microbial layer is firmly attached on the QCM gold surface, the sensor signals remain stable for about 6 h (from 10 to 16 h, II). At 16 h, we observe a new increase in both frequency and dissipation (yellow data, III) followed by a final stabilization

DOI: 10.1021/acssensors.9b01580
ACS Sens. 2019, 4, 3023−3033

(IV), which is possibly related to the biofilm reorganization and bond maturation. *D. acidovorans* growth on QCM has been repeated in five independent experiments, all showing similar 2-peak profiles in both frequency and dissipation sensorgrams. In addition, after 24 h of bacterial growth, frequency and dissipation signals stabilize at -101 ± 40 Hz and 40 ± 10 ppm, respectively.

Based on the QCM-D measurements, the dissipation/frequency ratio ($\Delta D/\Delta f$) can be used to highlight structural properties of the material on the QCM gold surface (Figure 2c: ΔD is plotted versus Δf). The steeper the $\Delta D/\Delta f$ profile, the softer the layer in contact with the QCM sensor surface. In the initial phases of the measurement (red data), adsorbed proteins from the culture medium form a compact layer on the sensor surface (the frequency shift Δf decreases without large variations in the energy dissipation of ΔD). However, cell adhesion and the first biofilm reorganization (blue data) result in a distinct regime in the *Df*-plot, corresponding to the formation of an increasingly soft film on the gold surface (blue data, I). This is followed by a progressive stabilization of cell adhesion on the QCM sensor surface, which results in a more compact bacterial structure (II). A similar trend can be observed in the later stage of biofilm development (yellow data, III and IV). This enhanced steeper profile indicates the formation of a structure softer than the initial one (blue data), which corresponds to the assembly and stabilization of the outer biofilm layer.

The mechanism described above (the captured two peaks and the growth stages highlighted in the QCM sensorgram) is further supported by optical microscopy (Figure 2d and Supporting Information, Movies SM1, SM2, and SM3), where *D. acidovorans* growing on a glass cover slip coated with a 15-nm-thick gold film is imaged for 24 h at 25 °C. Each video in SI corresponds to specific time intervals (i.e., 0−3 h for SM1, 3−8 h for SM2, and 8−24 h for SM3), showing time-lapsed images acquired on the sensor surface, with the aim of capturing the biofilm reorganization events occurring at about 7 h and 16 h, respectively. The real-time imaging of the biofilm growth reveals that the initial bacterial adhesion (from 0 to ≈5 h, Supporting Information, Movies SM1 and SM2) is followed by a microbial reorganization at ≈7 h (I, Supporting Information, Movie SM2). This observation supports the hypothesis that in this stage, cells are weakly bonded on the QCM surface. Indeed, the weak adhesion of the bacteria on the gold substrate, which is responsible for the broadness of the peak, results in the increase in both frequency and dissipation until 7 h, when both signals reach their maximum (Figure 2a). Between 7 and 12 h, the cells weakly adhering on the surface would go in and out of the focal plane, but eventually forming a biofilm firmly attached to the gold surface at ≈12 h (phase II), which causes a reduction in frequency. A similar but less pronounced second reorganization event is observed after roughly 16 h from the inoculum (III), corresponding to the second peak in the QCM sensorgrams, which is then followed by the final stabilization (IV). For more details, see Supporting Information, Movie SM3.

Morphological Characterization with AFM and Biomass Estimation with Crystal Violet Assay. After *D. acidovorans* grows on the QCM gold-coated quartz surface for 24 h, the resulting microbial biofilm is imaged by an atomic force microscope via tapping mode (Bruker, Dimension ICON3). This technique has proven useful for characterizing bacterial biofilm morphology and bacterial interactions and attachment on surfaces.[45] Areas of $20 \times 20\ \mu m^2$ (Figure 3a) and $10 \times 10\ \mu m^2$ (Figure 3b) reveal that bacteria and the EPS matrix constitute a

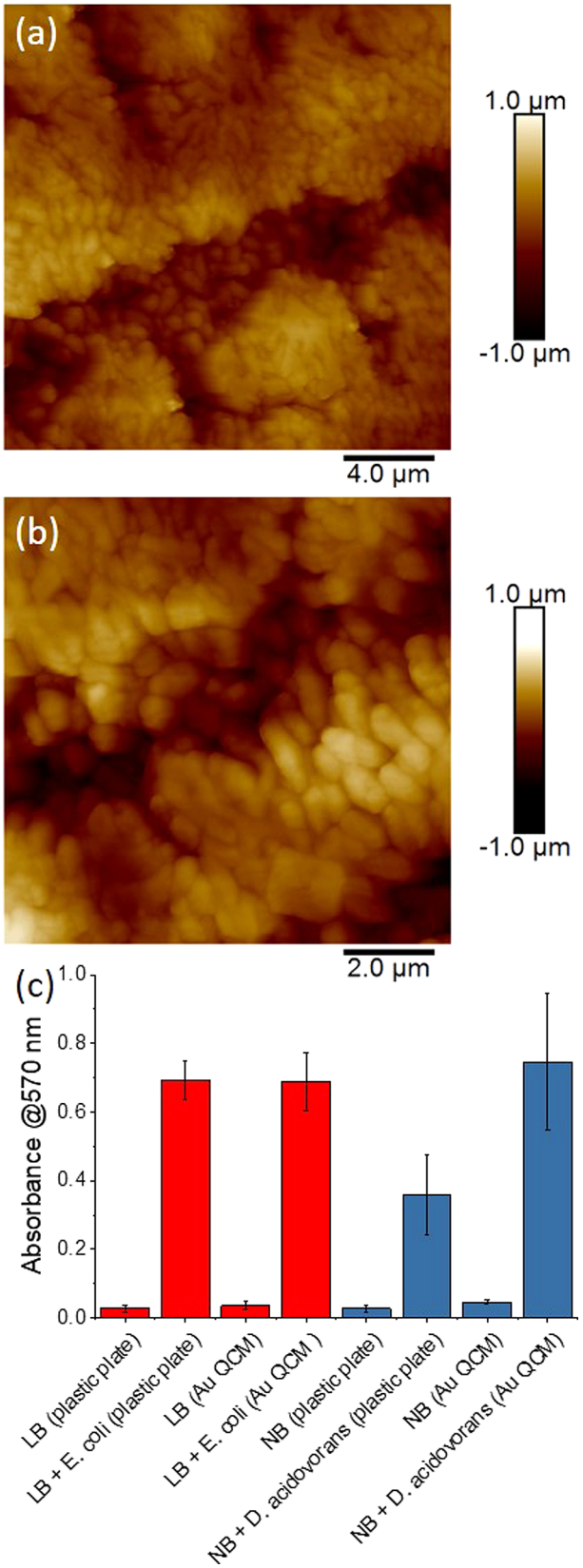

Figure 3. High-resolution AFM images of a 24 h *D. acidovorans* biofilm on a QCM gold surface. (a) $20 \times 20\ \mu m^2$ and (b) $10 \times 10\ \mu m^2$ scans. Stable and compact structures of bacteria and EPSs are observed. *D. acidovorans* biofilm formation has also been characterized using the conventional crystal violet assay, (c) while *E. coli* is used as a reference microorganism. These experiments have been performed on both plastic (well plate) and gold (QCM) surfaces. Both bacteria are grown

DOI: 10.1021/acssensors.9b01580
ACS Sens. 2019, 4, 3023−3033

Figure 3. continued

for 24 h before staining. While *E. coli* (red data) reaches the same biomass on both plastic and gold substrates, *D. acidovorans* (blue data) produces a more massive biofilm on gold. The absorbance values reported in the histogram correspond to three independent experiments, with the error bars denoting the standard deviation.

completely formed biofilm that covers the whole sensor surface. These results are critical to verify stable bacterial immobilization and biofilm formation on the gold sensor surface for further gold stress experiments.

The *D. acidovorans* biofilm formed after 24 h is also characterized using a crystal violet assay (Figure 3c), a staining methodology commonly used to evaluate the microbial biofilm biomass.[46] We compare the *D. acidovorans* biofilm (blue data) with the biofilm formed by *E. coli* (red data, used as a reference microorganism) formed on the gold sensor surface of the QCM and on a standard plastic 96-well plate.

Absorbance values at 570 nm (being directly proportional to the microbial biomass adhering on the surface) for the simple culture media (LB and NB for *E. coli* and *D. acidovorans*, respectively) are used as references. While *E. coli* reaches similar biomass on both plastic and gold substrates after 24 h, *D. acidovorans* forms a more massive biofilm on gold than on plastic. This can be explained by considering that *D. acidovorans* is usually isolated from the surfaces of gold nuggets.[8,47]

Identification of the Best Aqueous Solution for Monitoring Gold Biomineralization by *D. acidovorans* Biofilm. To identify the best sensing conditions for gold biomineralization by *D. acidovorans* biofilms, we evaluate the response of the bacteria when they are stressed with soluble gold ($AuCl_3$) in different culture media and buffer solutions. The biofilm formed on the QCM sensor is exposed to either NB, minimal medium (MM), or PBS. After the sensor stabilization, an aliquot of $AuCl_3$ stock solution is added to the sample to reach a final concentration of $AuCl_3$ at 100 μM (Table 1). While

Table 1. QCM Response of *D. acidovorans* Biofilm Stressed with 100 μM of $AuCl_3$ in NB, MM, and PBS

medium	Δf (Hz)	signal stabilization (h)
NB	-40 ± 20	N/A[a]
MM	-389 ± 144	≈12
PBS	-222 ± 32	≈14

[a]When the biomineralization is induced in NB, the QCM frequency signal continues to drop even after 20 h.

NB is a rich medium, MM provides only minimal nutrients for bacterial growth. On the other hand, PBS stabilizes the biofilm by maintaining a constant pH and ionic strength without providing nutrients.

When the *D. acidovorans* biofilm is stressed by Au^{3+} in NB, neither the quartz resonance frequency nor the energy dissipation signals stabilize within 20 h. In addition, since we are dealing with a nutrient-rich medium, it is not possible to discriminate the gold nanonugget formation from the microbial growth because both phenomena affect the quartz resonance frequency. Both PBS and MM provide a robust frequency shift and a reasonable frequency stabilization after 10 h from the introduction of $AuCl_3$ solution. In particular, the biofilm stressed with gold ions in MM results in a larger frequency shift compared to that obtained in PBS. Gold biomineralization also occurs more rapidly in MM (signal stabilization is achieved in 12 h in MM in comparison to ≈14 h in PBS). This enhanced biomineralization performance of *D. acidovorans* biofilm is related to the presence of nutrients in MM. However, the usage of MM also implies that the microorganisms have resources to multiply as well. This side-effect perturbs the resonance frequency of the QCM, thus increasing measurement error and making it more difficult to discriminate between biomineralization and bacterial growth. Therefore, among the tested solutions, PBS offers the best environment to accurately monitor biomineralization activity. Even though PBS does not contain nutrients to support cell growth, the biofilm still neutralizes gold (a consistent shift in frequency is recorded) and a frequency stabilization is reached after ≈14 h. Hereafter, experimental conditions (gold solutions in PBS and biomineralization in 14 h) will be used for further experiments.

Toxic Effect of $AuCl_3$ on *D. acidovorans* Biofilm. Since there is a limit of the amount of soluble gold that *D. acidovorans* can neutralize, gold toxicity on immobilized *D. acidovorans* has been evaluated by Live/Dead BacLight Bacterial Viability staining. This procedure is performed directly on the QCM gold surface after *D. acidovorans* biofilms are stressed with different $AuCl_3$ concentrations for 14 h (Figure 4). The assay involves two different fluorescent dyes (SYTO 9 and propidium iodide), which produce a strong green or red fluorescence signal, depending on whether the bacteria are alive or dead.

In our control experiments, the biofilm is exposed to PBS for 14 h (Figure 4a) and most of the cells are alive, producing largely green fluorescence. On the other hand, when the bacterial biofilm is stressed with 100 μM of $AuCl_3$ (Figure 4b), some red areas (due to dead cells) can be clearly identified. These experiments show that *D. acidovorans* have $AuCl_3$ concentrations up to about 50 μM in PBS without significant cell death. When the biofilm is stressed with higher concentrations of soluble gold, cell vitality decreases exponentially (Figure 4c). In particular, the fraction of living cells versus the concentration of $AuCl_3$ ($\alpha[Au^{3+}]$) can be described by a logistic-type equation

$$\alpha([Au^{3+}]) = \frac{A}{1 + e^{B([Au^{3+}]-C)}} \quad (1)$$

where A is the initial fraction of living cells on the gold surface of the QCM, B is a rate parameter defining the soluble gold toxicity for *D. acidovorans*, and C is the concentration at which cell vitality is half the maximum value. The best fit yields: $A = 0.883 \pm 0.004$, $B = 0.042 \pm 0.004$ μM^{-1}, and $C = 115 \pm 4$ μM. In particular, the concentration parameter C (half-maximal effective concentrations) is high when compared with bacteria exposed to other heavy metals (EC_{50}).[48] However, this result is reasonable considering that *D. acidovorans* has a specific detoxification mechanism to protect itself from soluble gold. This information is important in studying biomineralization because the healthier the bacteria, the more efficient the production of delftibactin and gold detoxification. The parameters obtained from the fit will be implemented in the analysis of QCM results reported in the next section.

Sensing Gold Biomineralization using QCM. The *D. acidovorans* biofilms formed over 24 h on the QCM gold sensor surfaces have been stressed by using $AuCl_3$ solutions with concentrations ranging from 0 to 100 μM in PBS. All of the QCM sensorgrams exhibit similar behaviors in both frequency and dissipation. Figure 5a shows an example of the biofilm response at 50 μM of $AuCl_3$. After the QCM signal stabilizes in PBS (≈1 h after the QCM chamber is filled with PBS), the

DOI: 10.1021/acssensors.9b01580
ACS Sens. 2019, 4, 3023−3033

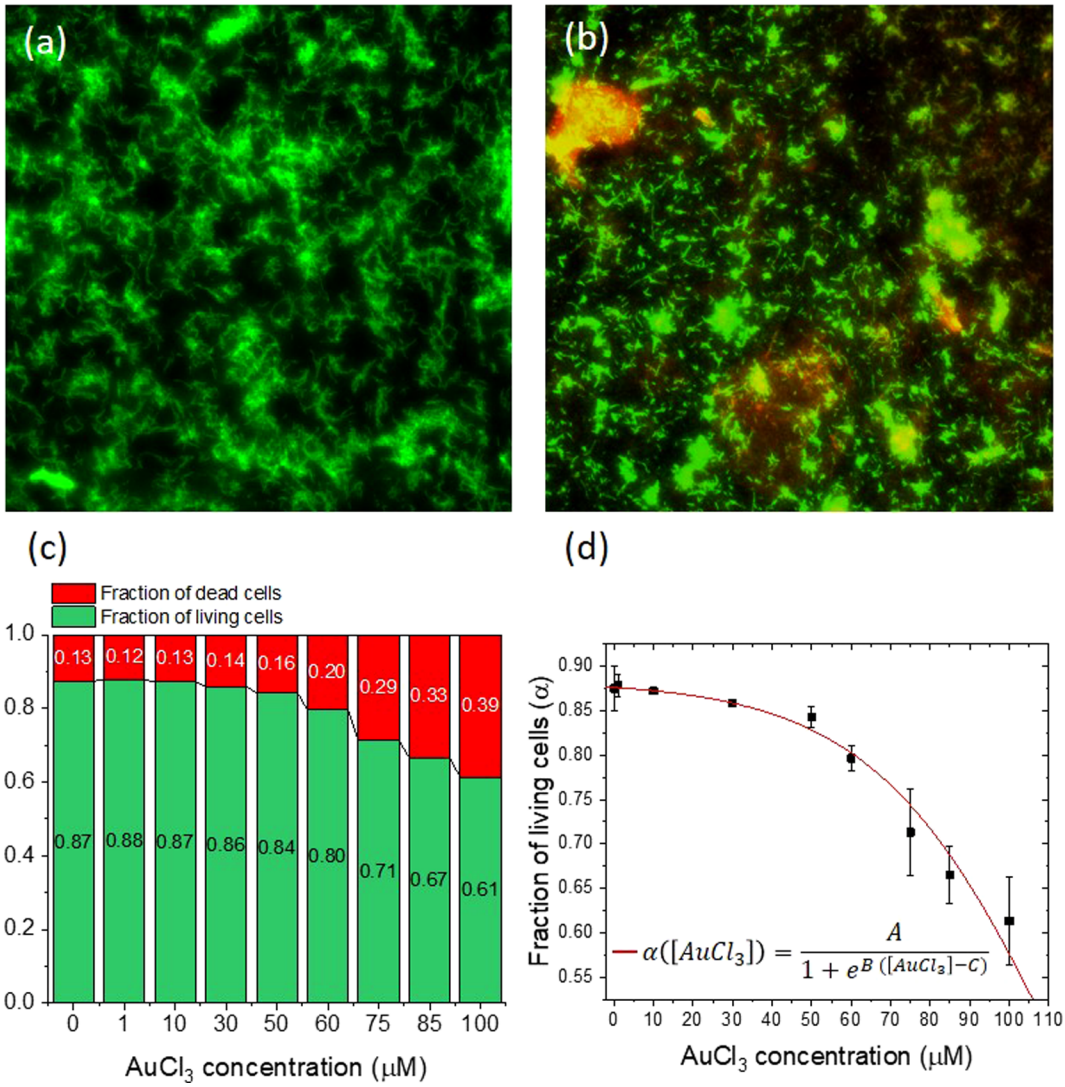

Figure 4. Viability staining for *D. acidovorans* stressed for 14 h with different concentrations of $AuCl_3$. The experiment is conducted using two different fluorescent dyes (SYTO 9 and propidium iodide). These emit in the green and red spectral regions and are specific for living and dead cells, respectively. (a) Control experiment performed by exposing the cells to PBS and (b) bacterial biofilm stressed with 100 μM of $AuCl_3$. *D. acidovorans* is able to survive by neutralizing the gold ions; however, the lack of nutrients (the measurement is performed in PBS) and the increasing concentration of Au result in a progressive decrease in cell vitality, as shown in (c). These experimental data are shown as black squares, with the best curve fit using a logistic-type relationship shown as a red solid curve (d). Each data point results from the analysis of three independent areas, with the error bars denoting the standard deviation.

bacterial biofilm is exposed to 50 μM of $AuCl_3$. The vertical dashed line highlights the addition of the soluble gold solution. Subsequently, progressive decreases in both resonance frequency of the quartz and energy dissipation are observed. These are compatible with the mass load on the QCM surface and the stiffening of the bacterial biofilm resulting from the biomineralization process. Indeed, *D. acidovorans* protects itself from the soluble gold by producing delftibactin, which chelates the Au^{3+} ions in a 1:1 ratio, forming an insoluble complex.[10,49] These delftibactin−Au complexes (AuD) precipitate on the QCM surface, damping the resonance frequency of the quartz. Most of the sensorgrams show a rather stable signal in both frequency and dissipation after about 14 h from the addition of the soluble gold solution. Therefore, gold biomineralization kinetics can be examined by analyzing the 14 h sensor responses of *D. acidovorans* biofilm (Figure 5b) on the QCM.

The sensor's frequency response can be modeled by considering that frequency variation (Δf) is directly proportional to the concentration of the AuD complex. This can be expressed using a Hill-type equation, a widely used model[50−52] to capture the response of cells against a certain stimulus

$$\Delta f \propto [\mathrm{AuD}] = K_{\mathrm{Au}}[\mathrm{D_{tot}}]\frac{[\mathrm{Au}^{3+}]}{K + [\mathrm{Au}^{3+}]}\Delta t \qquad (2)$$

where K_{Au} is the gold biomineralization rate expressed in h^{-1}, D_{tot} is the total amount of delftibactin produced, which is assumed to be a constant at equilibrium, K is the dissociation constant describing the affinity of the system for the Au^{3+} ions, and Δt is the duration of the experiment (i.e., 14 h in this case). Note that the amount of delftibactin produced ($[D_{\mathrm{tot}}]$) at each $AuCl_3$ concentration depends on the fraction of living cells in the biofilm. This can be obtained by eq 1 based on the viability staining results reported in the previous subsection. We multiply eq 1 with eq 2 to describe the frequency response due to the

DOI: 10.1021/acssensors.9b01580
ACS Sens. 2019, 4, 3023−3033

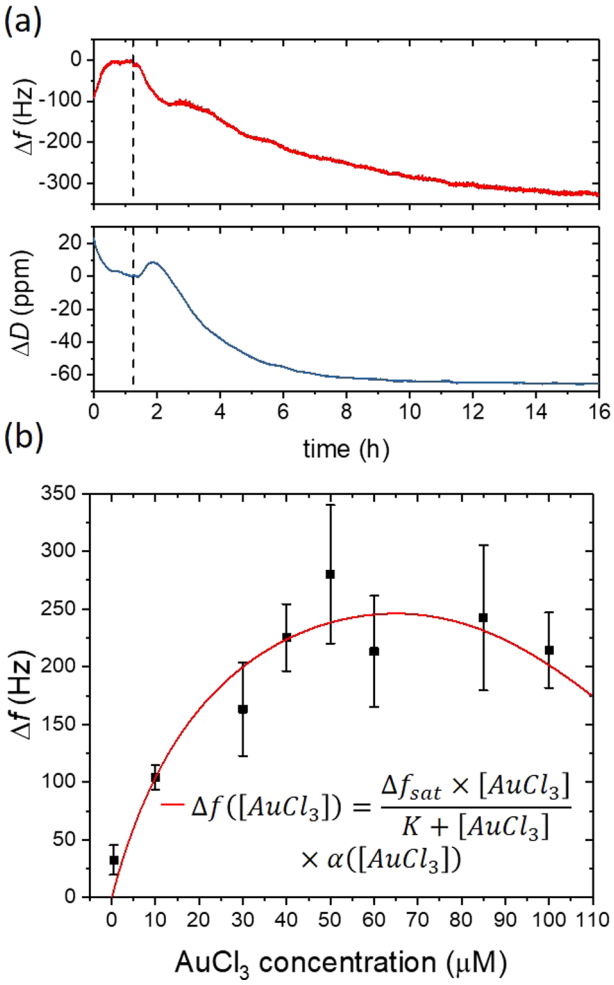

Figure 5. *D. acidovorans* response at several concentrations of $AuCl_3$ monitored using QCM. (a) The bacterial biofilm is first washed with PBS until the QCM resonance frequency stabilizes. The microorganisms are then stressed with soluble gold (50 μM $AuCl_3$), and both frequency and dissipation are monitored for more than 14 h. The vertical dashed line highlights the instant when 50 μM $AuCl_3$ is added to the system. The gold biomineralization and the subsequent gold nanonuggets production yield a progressive decrease in the resonant frequency of the gold coated quartz substrate. This is due to the deposition of gold complexes on the QCM sensor, functionalized by the bacterial biofilm. A decrease in the dissipation signal is also observed, which indicates a gradual stiffening of the material that is in contact with the QCM sensor surface due to the gold nanonugget formation. (b) Frequency response of the biofilm-covered QCM sensor surface at different concentrations of the soluble gold. Each data point corresponds to the average frequency shift from at least three independent experiments, with the error bars denoting the standard deviation. A modified Hill model incorporating the viability staining data is shown as a red solid curve.

biofilm on the QCM gold surface at various $AuCl_3$ concentrations (Figure 5b)

$$\Delta f = K_{Au}[D_{tot}]\Delta t \frac{[Au^{3+}]}{K + [Au^{3+}]}\alpha([Au^{3+}]) = \Delta f_{sat} \frac{[Au^{3+}]}{K + [Au^{3+}]} \frac{A}{1 + e^{B([Au^{3+}] - C)}} \quad (3)$$

where $\Delta f_{sat} = K_{Au}[D_{tot}]\Delta t$ is the maximum theoretical frequency shift possible by the system at saturating gold concentration without considering the toxic effect of gold, while A, B, and C are fitting parameters estimated by analyzing viability staining results ($A = 0.883 \pm 0.004$, $B = 0.042 \pm 0.004$ μM^{-1}, and $C = 115 \pm 4$ μM). Detailed description of the mathematical model can be found in SI. The best fit of the QCM responses gives values of $\Delta f_{sat} = 444 \pm 70$ Hz and $K = 27 \pm 8$ μM. The maximum of this curve corresponds to the concentration of $AuCl_3$ (≈ 64.7 μM) at which the biomineralization yield is maximized. Indeed, because of the intrinsic resistance of *D. acidovorans* against soluble gold, at this concentration, the toxicity of the $AuCl_3$ is not relevant enough to dampen the gold neutralization process. We should stress that the biomineralization process and gold quantification can be significantly improved by supplying a minimum amount of nutrients to the bacterial cells, so that more delftibactin can be produced to generate more nanonuggets. As discussed in the previous section, when the biomineralization is performed in MM rather than in PBS, the frequency shift due to the nanonugget formation is almost doubled (see Table 1). However, this condition will require an integrated microfluidic sensing platform to continuously supply the nutrients during sensing.

Confirmation of Gold Biomineralization via the TMB Assay. The 3,3',5,5'-tetramethylbenzidine (TMB) assay was used for independent confirmation that the biomineralization process has indeed occurred by the *D. acidovorans* biofilm (more details about this procedure can be found in the Materials and Methods Section). Briefly, the reaction between Au^{3+} and TMB molecules produces a strong increase in the absorbance at 654 nm, which is directly proportional to the concentration of free metal ions (Figure 6a and b). The calibration curve (Figure 6b) is obtained by plotting the absorbance at 654 nm against Au^{3+} concentrations. A linear relationship ($R^2 = 0.986$) in the range of 0−100 μM is obtained.

To verify depletion of free ionic gold due to biomineralization, *D. acidovorans* biofilm on the QCM surface is stressed with 60 μM of Au^{3+} and 10 μL aliquots of biofilm supernatant are collected at regular time intervals for 14 h. These samples are mixed with a TMB solution and absorption spectra between 500 and 800 nm are recorded (Figure 6c). The absorbance at 654 nm, and consequently the amount of free Au^{3+}, gradually reduces over time (Figure 6d) because of biomineralization by the bacteria, providing independent evidence of the biomineralization process.

CONCLUSIONS

We have demonstrated that QCM sensors provide a cheap, reliable, and user-friendly alternative to standard analytical techniques to quantify gold ions, and monitor biofilm formation and biomineralization by *D. acidovorans* in real time without any special sample treatment and in conditions resembling the native environment experienced by the microorganism. Since QCM is nondestructive, further microbiological investigations can be easily performed on the same sample. The complementary studies of *D. acidovorans* via QCM and AFM are in good agreement with the results provided by a standard colorimetric biomass assay, confirming the reliability of various techniques employed for characterizing bacterial biofilms in this work. The high temporal resolution and long-term stability provided by the QCM system allows the detailed real-time characterization of the gold biomineralization process for more than 14 h after the soluble gold is added to the system. In addition, measurement of the biofilm response at different $AuCl_3$ concentrations via QCM allows us to understand kinetics

DOI: 10.1021/acssensors.9b01580
ACS Sens. 2019, 4, 3023−3033

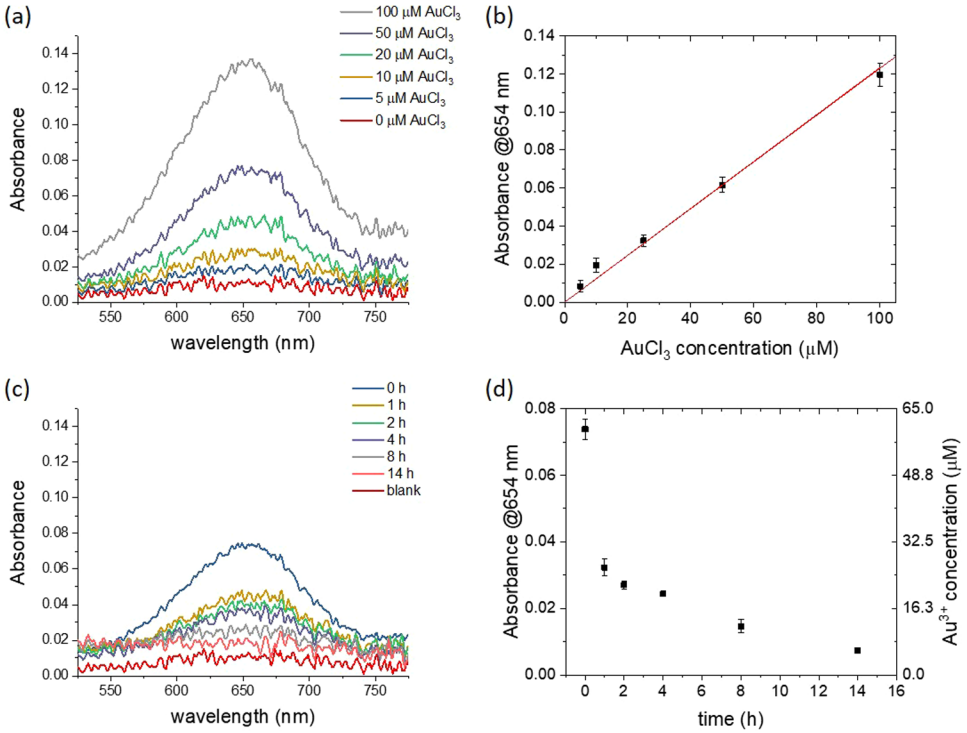

Figure 6. TMB assay to verify the gold biomineralized by *D. acidovorans* biofilm for 14 h. (a) Assay calibration performed on $AuCl_3$ samples in PBS. The reaction between gold ions and TMB molecules produces an increase in the absorbance at 654 nm, which can be used to quantify the concentration of the gold ions. (b) TMB assay calibration. (c) The *D. acidovorans* biofilm is stressed with 60 μM of $AuCl_3$ and samples of 10 μL are collected from the solution in the QCM cell. These are stored at 4 °C until the last volume is acquired at 14 h. Then, 2 μL of TMB solution is added to each sample and the absorbance spectrum in the visible range is recorded after 10 min. (d) The progressive decrease in absorbance at 654 nm documents the progressive depletion of the free ionic gold, neutralized by delftibactin in the form of nanonuggets. Each data point corresponds to the average of the absorbance of three different samples, while the error bars denote the standard deviation.

regulating the biomineralization performed by *D. acidovorans*, which can be helpful in optimizing sensing procedures, waste treatment, and bioremediation methods. Our studies have been performed at 25 °C. However, since temperature is critical in biological processes, further investigations will focus on the temperature dependence of biofilm formation and biomineralization. Since many bacteria and fungi are able to neutralize heavy metals in solution,[53−58] a reliable and cost-effective tool like QCM offers unique advantages in understanding and optimizing biomineralization processes for environmental applications such as sensing of heavy metals, gold prospection, and recovery.

■ ASSOCIATED CONTENT

Supporting Information

The Supporting Information is available free of charge on the ACS Publications website at DOI: 10.1021/acssensors.9b01580.

QCM device; real-time imaging of *D. acidovorans* growth on gold surface; imaging of QCM gold surface; crystal violet staining protocol; viability staining protocol; modeling of biomineralization kinetics (PDF)

Growth 0−3 h of *D. acidovorans* on a 15 nm gold layer evaporated on a glass cover slip (AVI)

Growth 3−8 h of *D. acidovorans* on a 15 nm gold layer evaporatedon a glass cover slip (AVI)

Growth 8−24 h of *D. acidovorans* on a 15 nm gold layer evaporatedon a glass cover slip (AVI)

■ AUTHOR INFORMATION

Corresponding Authors

*E-mail: riccardo.funari@oist.jp (R.F).
*E-mail: amy.shen@oist.jp (A.Q.S).

ORCID

Amy Q. Shen: 0000-0002-1222-6264

Notes

The authors declare no competing financial interest.

■ ACKNOWLEDGMENTS

We gratefully acknowledge the support of Okinawa Institute of Science and Technology Graduate University, with subsidy funding from the Cabinet Office, Government of Japan. A.Q.S. also acknowledges funding from the Japanese Society for the Promotion of Science Grants-in-Aid for Scientific Research (C) Grant JP17K06173 and Grants-in-Aid for Scientific Research (B) Grant JP18H01135. We also thank Kazumi Toda-Peters from the Micro/Bio/Nanofluidics unit at OIST, who provided his expertise in designing the custom components we used for bacteria growth.

■ REFERENCES

(1) Daniel, M.-C.; Astruc, D. Gold nanoparticles: assembly, supramolecular chemistry, quantum-size-related properties, and applications toward biology, catalysis, and nanotechnology. *Chem. Rev.* **2004**, *104*, 293−346.

(2) Wong, M.; Wu, S.; Deng, W. J.; Yu, X.; Luo, Q.; Leung, A.; Wong, C.; Luksemburg, W.; Wong, A. Export of toxic chemicals - A review of

DOI: 10.1021/acssensors.9b01580
ACS Sens. 2019, 4, 3023−3033

the case of uncontrolled electronic-waste recycling. *Environ. Pollut.* **2007**, *149*, 131−140.
(3) Habib, A.; Tabata, M. Oxidative DNA damage induced by HEPES (2-[4-(2-hydroxyethyl)-1-piperazinyl] ethanesulfonic acid) buffer in the presence of Au (III). *J. Inorg. Biochem.* **2004**, *98*, 1696−1702.
(4) Goebel, C.; Kubicka-Muranyi, M.; Tonn, T.; Gonzalez, J.; Gleichmann, E. Phagocytes render chemicals immunogenic: oxidation of gold (I) to the T cell-sensitizing gold (III) metabolite generated by mononuclear phagocytes. *Arch. Toxicol.* **1995**, *69*, 450−459.
(5) Park, J.; Choi, S.; Kim, T.-I.; Kim, Y. Highly selective fluorescence turn-on sensing of gold ions by a nanoparticle generation/C-I bond cleavage sequence. *Analyst* **2012**, *137*, 4411−4414.
(6) Nies, D. H. Microbial heavy-metal resistance. *Appl. Microbiol. Biotechnol.* **1999**, *51*, 730−750.
(7) Flemming, H.-C.; Wingender, J.; Szewzyk, U.; Steinberg, P.; Rice, S. A.; Kjelleberg, S. Biofilms: an emergent form of bacterial life. *Nat. Rev. Microbiol.* **2016**, *14*, 563.
(8) Rea, M. A.; Zammit, C. M.; Reith, F. Bacterial biofilms on gold grains−implications for geomicrobial transformations of gold. *FEMS Microb. Ecol.* **2016**, *92*, No. fiw082.
(9) Reith, F.; Brugger, J.; Zammit, C.; Nies, D.; Southam, G. Geobiological cycling of gold: from fundamental process understanding to exploration solutions. *Minerals* **2013**, *3*, 367−394.
(10) Johnston, C. W.; Wyatt, M. A.; Li, X.; Ibrahim, A.; Shuster, J.; Southam, G.; Magarvey, N. A. Gold biomineralization by a metallophore from a gold-associated microbe. *Nat. Chem. Biol.* **2013**, *9*, 241.
(11) Falkner, K. K.; Edmond, J. Gold in seawater. *Earth Planet. Sci. Lett.* **1990**, *98*, 208−221.
(12) Brar, S. K.; Hegde, K.; Pachapur, V. L. *Tools, Techniques and Protocols for Monitoring Environmental Contaminants*; Elsevier, 2019.
(13) Yüce, M.; Nazir, H.; Dönmez, G. An advanced investigation on a new algal sensor determining Pb (II) ions from aqueous media. *Biosens. Bioelectron.* **2010**, *26*, 321−326.
(14) Amaro, F.; Turkewitz, A. P.; Martín-González, A.; Gutiérrez, J. C. Functional GFP-metallothionein fusion protein from Tetrahymena thermophila: a potential whole-cell biosensor for monitoring heavy metal pollution and a cell model to study metallothionein overproduction effects. *BioMetals* **2014**, *27*, 195−205.
(15) Leth, S.; Maltoni, S.; Simkus, R.; Mattiasson, B.; Corbisier, P.; Klimant, I.; Wolfbeis, O. S.; Csöregi, E. Engineered bacteria based biosensors for monitoring bioavailable heavy metals. *Electroanalysis* **2002**, *14*, 35−42.
(16) Corbisier, P.; van der Lelie, D.; Borremans, B.; Provoost, A.; de Lorenzo, V.; Brown, N. L.; Lloyd, J. R.; Hobman, J. L.; Csöregi, E.; Johansson, G.; et al. Whole cell-and protein-based biosensors for the detection of bioavailable heavy metals in environmental samples. *Anal. Chim. Acta* **1999**, *387*, 235−244.
(17) Verma, N.; Singh, M. A Bacillus sphaericus based biosensor for monitoring nickel ions in industrial effluents and foods. *J. Anal. Methods Chem.* **2006**, *2006*, No. 83427.
(18) Ammann, A. A. Inductively coupled plasma mass spectrometry (ICP MS): a versatile tool. *J. Mass Spectrom.* **2007**, *42*, 419−427.
(19) Sauerbrey, G. The use of quarts oscillators for weighing thin layers and for microweighing. *Z. Phys.* **1959**, *155*, 206−222.
(20) Ballantine, D., Jr.; White, R. M.; Martin, S. J.; Ricco, A. J.; Zellers, E.; Frye, G.; Wohltjen, H. *Acoustic Wave Sensors: Theory, Design and Physico-Chemical Applications*; Elsevier, 1996.
(21) Cho, N.-J.; Kanazawa, K. K.; Glenn, J. S.; Frank, C. W. Employing two different quartz crystal microbalance models to study changes in viscoelastic behavior upon transformation of lipid vesicles to a bilayer on a gold surface. *Anal. Chem.* **2007**, *79*, 7027−7035.
(22) Feng, K.; Li, J.; Jiang, J.-H.; Shen, G.-L.; Yu, R.-Q. QCM detection of DNA targets with single-base mutation based on DNA ligase reaction and biocatalyzed deposition amplification. *Biosens. Bioelectron.* **2007**, *22*, 1651−1657.
(23) Tombelli, S.; Mascini, M.; Turner, A. P. Improved procedures for immobilisation of oligonucleotides on gold-coated piezoelectric quartz crystals. *Biosens. Bioelectron.* **2002**, *17*, 929−936.
(24) Funari, R.; Della Ventura, B.; Schiavo, L.; Esposito, R.; Altucci, C.; Velotta, R. Detection of parathion pesticide by quartz crystal microbalance functionalized with UV-activated antibodies. *Anal. Chem.* **2013**, *85*, 6392−6397.
(25) Funari, R.; Della Ventura, B.; Carrieri, R.; Morra, L.; Lahoz, E.; Gesuele, F.; Altucci, C.; Velotta, R. Detection of parathion and patulin by quartz-crystal microbalance functionalized by the photonics immobilization technique. *Biosens. Bioelectron.* **2015**, *67*, 224−229.
(26) Pavey, K.; Barnes, L.-M.; Hanlon, G.; Olliff, C.; Ali, Z.; Paul, F. A rapid, non-destructive method for the determination of Staphylococcus epidermidis adhesion to surfaces using quartz crystal resonant sensor technology. *Lett. Appl. Microbiol.* **2001**, *33*, 344−348.
(27) Heitmann, V.; Wegener, J. Monitoring cell adhesion by piezoresonators: impact of increasing oscillation amplitudes. *Anal. Chem.* **2007**, *79*, 3392−3400.
(28) Alexander, T. E.; Lozeau, L. D.; Camesano, T. A. QCM-D Characterization of Time-Dependence of Bacterial Adhesion. *Cell Surf.* **2019**, No. 100024.
(29) Olsson, A. L.; Van der Mei, H. C.; Busscher, H. J.; Sharma, P. K. Influence of cell surface appendages on the bacterium- substratum interface measured real-time using QCM-D. *Langmuir* **2009**, *25*, 1627−1632.
(30) Gutman, J.; Walker, S. L.; Freger, V.; Herzberg, M. Bacterial attachment and viscoelasticity: physicochemical and motility effects analyzed using quartz crystal microbalance with dissipation (QCM-D). *Environ. Sci. Technol.* **2013**, *47*, 398−404.
(31) Marcus, I. M.; Herzberg, M.; Walker, S. L.; Freger, V. Pseudomonas aeruginosa attachment on QCM-D sensors: the role of cell and surface hydrophobicities. *Langmuir* **2012**, *28*, 6396−6402.
(32) Reipa, V.; Almeida, J.; Cole, K. D. Long-term monitoring of biofilm growth and disinfection using a quartz crystal microbalance and reflectance measurements. *J. Microbiol. Methods* **2006**, *66*, 449−459.
(33) Nivens, D. E.; Chambers, J. Q.; Anderson, T. R.; White, D. C. Long-term, on-line monitoring of microbial biofilms using a quartz crystal microbalance. *Anal. Chem.* **1993**, *65*, 65−69.
(34) Ziemba, C.; Shabtai, Y.; Piatkovsky, M.; Herzberg, M. Cellulose effects on morphology and elasticity of Vibrio fischeri biofilms. *npj Biofilms Microbiomes* **2016**, *2*, No. 1.
(35) Ferrando Chavez, D. L.; Nejidat, A.; Herzberg, M. Viscoelastic properties of extracellular polymeric substances can strongly affect their washing efficiency from reverse osmosis membranes. *Environ. Sci. Technol.* **2016**, *50*, 9206−9213.
(36) Xia, X.; Zhang, J.; Sawall, T. A simple colorimetric method for the quantification of Au (III) ions and its use in quantifying Au nanoparticles. *Anal. Methods* **2015**, *7*, 3671−3675.
(37) Sule, P.; Wadhawan, T.; Carr, N. J.; Horne, S. M.; Wolfe, A. J.; Prüβ, B. M. A combination of assays reveals biomass differences in biofilms formed by *Escherichia coli* mutants. *Lett. Appl. Microbiol.* **2009**, *49*, 299−304.
(38) Xu, Z.; Liang, Y.; Lin, S.; Chen, D.; Li, B.; Li, L.; Deng, Y. Crystal violet and XTT assays on Staphylococcus aureus biofilm quantification. *Curr. Microbiol.* **2016**, *73*, 474−482.
(39) Schofield, A. L.; Rudd, T. R.; Martin, D. S.; Fernig, D. G.; Edwards, C. Real-time monitoring of the development and stability of biofilms of Streptococcus mutans using the quartz crystal microbalance with dissipation monitoring. *Biosens. Bioelectron.* **2007**, *23*, 407−413.
(40) Olsson, A. L.; Mitzel, M. R.; Tufenkji, N. QCM-D for non-destructive real-time assessment of Pseudomonas aeruginosa biofilm attachment to the substratum during biofilm growth. *Colloids Surf., B* **2015**, *136*, 928−934.
(41) Dybwad, G. A sensitive new method for the determination of adhesive bonding between a particle and a substrate. *J. Appl. Phys.* **1985**, *58*, 2789−2790.
(42) Geng, J.; Henry, N. *Bacterial Adhesion*; Springer, 2011; pp 315−331.
(43) Utada, A. S.; Bennett, R. R.; Fong, J. C.; Gibiansky, M. L.; Yildiz, F. H.; Golestanian, R.; Wong, G. C. Vibrio cholerae use pili and flagella synergistically to effect motility switching and conditional surface attachment. *Nat. Commun.* **2014**, *5*, No. 4913.

DOI: 10.1021/acssensors.9b01580
ACS Sens. 2019, 4, 3023−3033

(44) Tarnapolsky, A.; Freger, V. Modeling QCM-D Response to Deposition and Attachment of Microparticles and Living Cells. *Anal. Chem.* **2018**, *90*, 13960−13968.
(45) Wright, C. J.; Shah, M. K.; Powell, L. C.; Armstrong, I. Application of AFM from microbial cell to biofilm. *Scanning* **2010**, *32*, 134−149.
(46) Feoktistova, M.; Geserick, P.; Leverkus, M. Crystal violet assay for determining viability of cultured cells. *Cold Spring Harbor Protoc.* **2016**, *2016*, No. pdb-prot087379.
(47) Reith, F.; Fairbrother, L.; Nolze, G.; Wilhelmi, O.; Clode, P. L.; Gregg, A.; Parsons, J. E.; Wakelin, S. A.; Pring, A.; Hough, R.; Southam, G.; Brugger, J. Nanoparticle factories: Biofilms hold the key to gold dispersion and nugget formation. *Geology* **2010**, *38*, 843−846.
(48) Rathnayake, I.; Megharaj, M.; Krishnamurti, G.; Bolan, N. S.; Naidu, R. Heavy metal toxicity to bacteria−Are the existing growth media accurate enough to determine heavy metal toxicity. *Chemosphere* **2013**, *90*, 1195−1200.
(49) Wyatt, M. A.; Johnston, C. W.; Magarvey, N. A. Gold nanoparticle formation via microbial metallophore chemistries. *J. Nanopart. Res.* **2014**, *16*, 2212.
(50) Weiss, J. N. The Hill equation revisited: uses and misuses. *FASEB J.* **1997**, *11*, 835−841.
(51) Goutelle, S.; Maurin, M.; Rougier, F.; Barbaut, X.; Bourguignon, L.; Ducher, M.; Maire, P. The Hill equation: a review of its capabilities in pharmacological modelling. *Fundam. Clin. Pharmacol.* **2008**, *22*, 633−648.
(52) Kurganov, B.; Lobanov, A.; Borisov, I.; Reshetilov, A. Criterion for Hill equation validity for description of biosensor calibration curves. *Anal. Chim. Acta* **2001**, *427*, 11−19.
(53) Maity, J. P.; Chen, G.-S.; Huang, Y.-H.; Sun, A.-C.; Chen, C.-Y. Ecofriendly Heavy Metal Stabilization: Microbial Induced Mineral Precipitation (MIMP) and Biomineralization for Heavy Metals within the Contaminated Soil by Indigenous Bacteria. *Geomicrobiol. J.* **2019**, *36*, 612−623.
(54) Romero-Nunez, A.; Gonzalez, G.; Moreno, A.; Cuellar-Cruz, M. Biomineralization and biosynthesis of nanocrystalline materials and selective uptake of toxic metals controlled by five types of Candida species. *CrystEngComm* **2019**, *21*, 2585−2595.
(55) Zhang, K.; Xue, Y.; Xu, H.; Yao, Y. Lead removal by phosphate solubilizing bacteria isolated from soil through biomineralization. *Chemosphere* **2019**, *224*, 272−279.
(56) Kim, J.-H.; Lee, J.-Y. An optimum condition of MICP indigenous bacteria with contaminated wastes of heavy metal. *J. Mater. Cycles Waste Manage.* **2019**, *21*, 239−247.
(57) Khadim, H. J.; Ammar, S. H.; Ebrahim, S. E. Biomineralization based remediation of cadmium and nickel contaminated wastewater by ureolytic bacteria isolated from barn horses soil. *Environ. Technol. Innovation* **2019**, *14*, 100315.
(58) Li, M.; Cheng, X.; Guo, H. Heavy metal removal by biomineralization of urease producing bacteria isolated from soil. *Int. Biodeterior. Biodegrad.* **2013**, *76*, 81−85.

DOI: 10.1021/acssensors.9b01580
ACS Sens. 2019, 4, 3023−3033